White light emission from p-doped quaternary (AllnGa)N-based superlattices: Theoretical calculations for the cubic phase

S. C. P. Rodrigues, M. N. d'Eurydice, G. M. Sipahi, L. M. R. Scolfaro, and E. F. da Silva

Citation: Journal of Applied Physics 101, 113706 (2007); doi: 10.1063/1.2737968

View online: https://doi.org/10.1063/1.2737968

View Table of Contents: http://aip.scitation.org/toc/jap/101/11

Published by the American Institute of Physics



White light emission from *p*-doped quaternary (AllnGa)N-based superlattices: Theoretical calculations for the cubic phase

S. C. P. Rodrigues

Departamento de Física, Universidade Federal Rural de Pernambuco, R. Dom Manoel de Medeiros, s/n - Dois Irmãos, 52171-900 Recife, Pernambuco, Brazil

M. N. d'Eurydice and G. M. Sipahi

Instituto de Física de São Carlos, Universidade de São Paulo, CP 369, 013560-970 São Carlos, SP, Brazil

L. M. R. Scolfaro^{a)}

Instituto de Física, Universidade de São Paulo, CP 66318, 05315-970 São Paulo, SP, Brazil

E. F. da Silva, Jr.

Departamento de Física, Universidade Federal de Pernambuco, 50670-901 Recife, Pernambuco, Brazil

(Received 30 November 2006; accepted 30 March 2007; published online 11 June 2007)

light structure and emission spectra from *p*-doped $(Al_XIn_{1-X-Y}Ga_Y)N/(Al_xIn_{1-X-Y}Ga_Y)N$ superlattices (SLs) in the zinc blend (cubic) structure are investigated by means of self-consistent calculations which are performed within the $\mathbf{k} \cdot \mathbf{p}$ approach. Exchange and correlation effects, within the generated hole gas, are taken into account in the local density approximation. The calculated luminescence and absorption spectra show that light emission, due to recombination from confined states in the wells, is redshifted in the doped systems compared undoped SLs. It is demonstrated that p-doped to $(Al_xIn_{1-x-y}Ga_y)N/(Al_xIn_{1-x-y}Ga_y)N$ SLs give rise to the feasibility of achieving white light emission, through emissions covering all the visible region spectra, from violet to red. These findings provide important guidelines for the interpretation of forthcoming experiments in quaternary group-III nitride-based alloy systems, and for the design of advanced optoelectronic devices based on these alloys. © 2007 American Institute of Physics. [DOI: 10.1063/1.2737968]

I. INTRODUCTION

The group-III nitrides, and their ternary and quaternary alloys have been extensively investigated in the past years, mainly due to their importance toward developing electronic and optoelectronic advanced device technology. Nowadays, one of the most important applications of optoelectronic devices is the design and engineering of light-emitting diodes (LEDs) working from ultraviolet (UV) through infrared (IR), thus covering the whole visible spectrum. Among the III-nitrides and their alloys, the most important characteristics for LEDs driving the rapid advances in this area are high brightness, high quantum efficiency, high flexibility, long-lifetime, and low power consumption. ^{1,2}

In order to be able to reach both extrema of the visible spectrum, the use of quaternary $(Al_xIn_{1-x-y}Ga_y)N$ alloys has recently increased.³ The $(Al_xIn_{1-x-y}Ga_y)N$ alloy allows for independent control of lattice constant and band gap energy, which gives great flexibility in the design of devices. Another interesting feature is that this alloy is responsible for higher emission intensities than the ternary (AlGa)N alloy with the absence of In.³ Through the quaternary $(Al_xIn_{1-x-y}Ga_y)N$, it is possible to reach the near-UV region, which leads to a better adjustment of white light emission through the mixing of different emission wavelengths with adequate intensities.

Highly conductive p-type III-nitride layers are of crucial

In this work we address the possibility of obtaining quaternary from p-doped emission $(Al_XIn_{1-X-Y}Ga_Y)N/(Al_xIn_{1-x-y}Ga_y)N$ SLs, by properly choosing the x and y contents in the wells and the acceptor doping concentration N_A in the barriers. We assumed the quaternary alloys in the zinc blend (cubic) structure for the calculations. Although most of the work in nitrides has been done for hexagonal (wurtzite) structures, research efforts toward a more complete understanding of the cubic nitridederived structures have increased in the last few years.⁸⁻¹⁰ Successful growth of quaternary cubic-(Al_xIn_{1-x-v}Ga_v)N layers lattice matched to GaN have been recently demonstrated. 11 The absence of polarization fields in the cubic-III nitrides may be advantageous for some device applications.

Typical values are taken for the Al and Ga contents in the quaternary $(Al_XIn_{1-X-Y}Ga_Y)N$ alloy forming the barrier, X=0.20, Y=0.75; hence, the In concentration is 5%, and enough confinement in the wells is achieved. We consider short-period SLs, with fixed barrier and well thicknesses of 8

importance, in particular, for the production of LEDs. Although the control of p-doping in these materials is still a subject of discussion, remarkable progress has been achieved.^{3–5} One method that has been used to increase the p-dopant concentration is the superlattice (SL) approach, which allows doping to reach values as high as $\approx 10^{19}$ cm⁻³ for the hole's charge densities.^{6,7}

^{a)}Corresponding author; electronic mail: scolfaro@if.usp.br

and 3 nm, respectively, so the wells are compressively strained. Therefore, In segregation effects, which take place in the bulk III-nitride alloys, for high In contents, can be suppressed by biaxial strain as theoretically predicted and measured for cubic-(InGa)N. ¹²

Here, we show that it is possible to achieve light emission which covers the visible spectrum from violet to red, by properly choosing the alloy contents x and y in p-doped $(Al_{0.20}In_{0.05}Ga_{0.75})N/(Al_xIn_{1-x-y}Ga_y)N$ SLs. The emissions originated in the confined states recombination in the wells are found to be redshifted for the doped SLs as compared to the undoped case. This is a consequence of the self-consistent potential bending induced by the presence of free holes. If such SLs, or combinations of them are conveniently designed, white light emission can be easily obtained through the use of quaternary III-nitride based alloys. This is specially true after the recent progress observed in the production of high-In concentration nitride alloys, which are also necessary in order to reach the IR region.

II. METHODS OF CALCULATION

The calculations were carried out by means of a self-consistent $\mathbf{k} \cdot \mathbf{p}$ approach, which solves the 8 × 8 Kane multi-band effective mass equation (EME) together with the Poisson equation for the hole's charge distribution. ¹³ An infinite superlattice (SL) formed of square wells and barriers along the (001) direction is assumed.

The multiband EME is represented with respect to plane waves with vectors $K=(2\pi/d)l$ (l being an integer and d the SL period) equal to the reciprocal SL vector. The rows and columns of the 8×8 Kane Hamiltonian refer to the Blochtype eigenfunctions $|jm_j\mathbf{k}\rangle$ of Γ_8 heavy- and light-hole bands, Γ_7 spin-orbit-split-hole band, and Γ_6 conduction band; \mathbf{k} denotes a vector in the first SL Brillouin zone (BZ).

By expanding the EME with respect to plane waves (z|K) one is able to represent this equation with respect to Bloch functions $(\mathbf{r}|jm_j\vec{\mathbf{k}}+K\mathbf{e_z})$. For a Bloch-type eigenfunction $(z|E\mathbf{k})$ of the SL of energy E and wave vector \mathbf{k} , the EME takes the form

$$\sum_{j'm'_jK'} \left(jm_j \mathbf{k} K | H_0 + H_s + V_{het} + V_A + V_H + V_{xc} | j'm'_j \mathbf{k} K' \right)$$

$$\times \left(j'm'_j \mathbf{k} K' | E\mathbf{k} \right) = E(\mathbf{k}) \left(jm_j \mathbf{k} K | E\mathbf{k} \right), \tag{1}$$

where H_0 is the effective kinetic energy operator, H_s is the strain operator, V_{het} is the valence- (or conduction-band) discontinuity potential, which is diagonal with respect to jm_j , $j'm'_j$, V_A is the ionized acceptor charge distribution potential, V_H is the Hartree potential due to the hole's charge distribution, and V_{xc} is the exchange-correlation potential for the hole gas taken within LDA.

The Coulomb potential, $V_C(=V_A+V_H)$, is obtained by means of the self-consistent procedure, by solving the Poisson equation in the reciprocal space, i.e.,

$$(K|V_C|K') = \frac{4\pi e^2}{\varepsilon} \frac{1}{|K - K'|^2} [(K|N_A(z)|K') - (K|p(z)|K')], \tag{2}$$

with ε being the dielectric constant, e the electron charge, $N_A(z)$ the ionized acceptors concentration, and p(z) being the hole's charge distribution, which is given by

$$p(z) = \sum_{\substack{jm_j \mathbf{k} \in \text{empty states}}} |(zs|jm_j \mathbf{k})|^2,$$
(3)

where s is the spin coordinate. The strain operator H_s is determined by following our previous works. ¹³

From the calculated eigenstates, we can determine the luminescence and absorption spectra of the SL by using the following general expression:¹⁴

$$I(\omega) = \frac{2\hbar\omega^3}{c} \frac{e^2}{m_0 c^2} \sum_{\mathbf{k}} \sum_{n_e} \sum_{\substack{n_q \\ g = hh.lh.so}} f_{n_e n_q}(\mathbf{k}) N_{n_e \mathbf{k}} \left[1 - N_{n_q \mathbf{k}} \right]$$

$$\times \frac{\gamma}{\pi \left[E_{n_e}(\mathbf{k}) - E_{n_q}(\mathbf{k}) - \hbar\omega\right]^2 + \gamma^2},\tag{4}$$

where m_0 is the electron mass, ω is the incident radiation frequency, γ is the emission broadening (assumed as constant and equal to 10 meV), E_{n_e} and E_{n_q} are the energies associated with n_e and n_q , respectively, the electron and hole states involved in the transition. The occupation functions $N_{n_e \mathbf{k}}$ and $[1-N_{n_q \mathbf{k}}]$ are the Fermi-type occupation functions for states in the conduction- and valence band, respectively.

For the calculation of luminescence (absorption) spectra, the sum in Eq. (4) is performed over the occupied states in the conduction (valence) band, and unoccupied states in the valence (conduction) band.

The oscillator strength, $f_{n_{\rho}n_{q}}(\mathbf{k})$, is given by

$$f_{n_e n_q}(\mathbf{k}) = \frac{2}{m_0} \sum_{\sigma_e \sigma_a} \frac{|\langle n_e \sigma_e \mathbf{k} | p_x | n_q \sigma_q \mathbf{k} \rangle|^2}{E_{n_e}(\mathbf{k}) - E_{n_a}(\mathbf{k})},$$
 (5)

where p_x is the dipole momentum in the x-direction, σ_e and σ_q denote the spin values for electron and holes, respectively.

All the parameters used in the present calculations are shown in Table I. We used the expression provided in Ref. 15 for the quaternary $(Al_xIn_{1-x-y}Ga_y)N$ band gap energy dependence on the alloy contents, x and y. For all the other quantities, we interpolated linearly between the values for the binaries, AlN, GaN, and InN. The temperature dependence of band gap energies was evaluated through the Varshni analytical expression as applied for GaN (see Ref. 16).

We should mention that the more recent reported values for the InN band gap energy are $0.6-0.7 \text{ eV}.^{17-21}$ Although in the present calculations we adopted the value of $E_g(\text{InN}) = 0.9 \text{ eV}$ (Table I), we point out that if any value < 0.9 eV is assumed, less In content in the quaternary alloy which forms the well is needed to reach the IR region, and our conclusions remain unaltered.

TABLE I. Values of the parameters used in the self-consistent calculations of the *p*-doped cubic $(Al_{0.20}In_{0.05}Ga_{0.75})N/(Al_xIn_{1-x-y}Ga_y)N$ SLs. Data extracted from Refs. 14 and 22–24. We mention that the more recent reported values for the InN band gap energy are $\approx 0.6-0.7$ eV. (Refs. 17–21). However, the use of a smaller value than the one used here does not change our conclusions.

	GaN	InN	AlN	
γ_1	2.96	3.77	1.54	
γ_2	0.90	1.33	0.42	
γ_3	1.20	1.60	0.64	
$\Delta_{so}({ m meV})$	17	3	19	
a(Å)	4.552	5.030	4.380	
m_{hh}^*	0.86	0.84	1.44	
m_{lh}^*	0.21	0.16	0.42	
m_{so}^*	0.30	0.24	0.63	
m_e^*	0.15	0.10	0.067	
$E_g^{\Gamma}(eV)$	3.3	0.9	5.94	
$a_g(eV)$	-8.50	-12.98	-9.40	
$2/3D_u(eV)$	1.6	1.2	1.5	
$C_{11}(\text{GPa})$	293	187	304	
<i>C</i> ₁₂ (GPa)	159	125	160	

III. RESULTS AND DISCUSSION

In this section we discuss the results of p-type doped quaternary ($Al_{0.20}In_{0.05}Ga_{0.75}$)N/($Al_xIn_{1-x-y}Ga_y$)N SLs, for a set of different alloy contents, x and y, and two distinct ionized acceptor concentrations, $N_A = 5 \times 10^{18}$ cm⁻³ and $N_A = 1 \times 10^{19}$ cm⁻³. The acceptor doping distribution is assumed to be uniform in the quaternary alloy which forms the barriers, and are all ionized, thus the holes charge densities $p = N_A$. For comparison, we also discuss the results for the systems in an undoped condition. In all SLs studied here, the wells are compressively strained.

Figure 1 shows the self-consistent band structure, along the high symmetry lines ΓZ and Δ , obtained for a uniformly p-doped barrier of an $(Al_{0.20}In_{0.05}Ga_{0.75})N/(In_{0.65}Ga_{0.35})N$ SL, with $N_A=1\times 10^{19}$ cm⁻³. Only the first eight valence-band levels and the first two conduction-band levels are presented. The hole levels are labeled according to their main character at the Γ -point. The notation "soi-lhi" ("lhi-soi") means that the mixing character of band i is dominated by the split-off hole band, so (light-hole band, lh). The energy zero was placed at the top of the Coulomb potential at the $(Al_{0.20}In_{0.05}Ga_{0.75})N$ barrier. No miniband dispersion (along the ΓZ -direction) is seen; thus the wells are isolated. The first heavy-hole level, hh1, is found to be occupied. The Fermi level lies within the second heavy-hole band, hh2, which is only slightly occupied.

In Fig. 2 we present the calculated photoluminescence (PL) spectra at T=2 K for p-doped (Al_{0.20}In_{0.05}Ga_{0.75})N/(Al_xIn_{1-x-y}Ga_y)N SLs, where the x and y contents assume the values depicted in Table II. The ionized acceptor concentrations are $N_A=0$ (undoped), $N_A=5 \times 10^{18}$ cm⁻³, and $N_A=1 \times 10^{19}$ cm⁻³. The values taken for x and y are such that allow coverage of a wide energy range, from the red to the violet region of the electromagnetic spectrum.

In order to better visualize the energy shifts due to the changes in N_A , and see detailed structures of the peaks, we

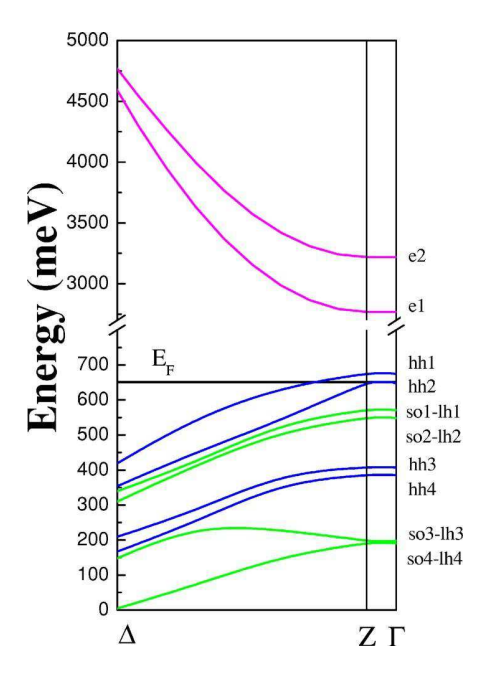


FIG. 1. Conduction- and valence-band structure, along the SL symmetry lines Γ -Z (growth axis) and Δ (perpendicular to the growth axis) of a p-doped (Al $_{0.20}$ In $_{0.05}$ Ga $_{0.75}$)N/In $_{0.65}$ Ga $_{0.35}$ N SL (note, the Al content x=0), which gives rise to transitions in the red part of the electromagnetic spectrum. The ionized acceptor concentration is N_A =1 × 10¹⁹ cm⁻³. Two electron levels, e1 and e2, and several hole levels hh1, hh2, sol-lh1, so2-lh2, hh3, hh4, so3-lh3, and so4-lh4, are shown (see the text for notation). The energy zero was taken at the top of the Coulomb potential at the (Al $_{0.20}$ In $_{0.05}$ Ga $_{0.75}$)N barrier. The Fermi level, E $_F$, is shown by the horizontal solid line

show in Fig. 3 the theoretical PL spectra depicted in Fig. 2, but in a two-dimensional view, ascribing different lines to distinguish the three acceptor doping cases: undoped (dotted lines), $N_A = 5 \times 10^{18}$ cm⁻³ (solid lines), and $N_A = 1 \times 10^{19}$ cm⁻³ (dashed lines). As N_A increases, a redshift of the PL peaks seen in Fig. 3 is clearly observed. This is due to the potential bending shape induced by the presence of free holes in the SL wells, which lowers the recombination transition energies. The second peak which is seen on the right of

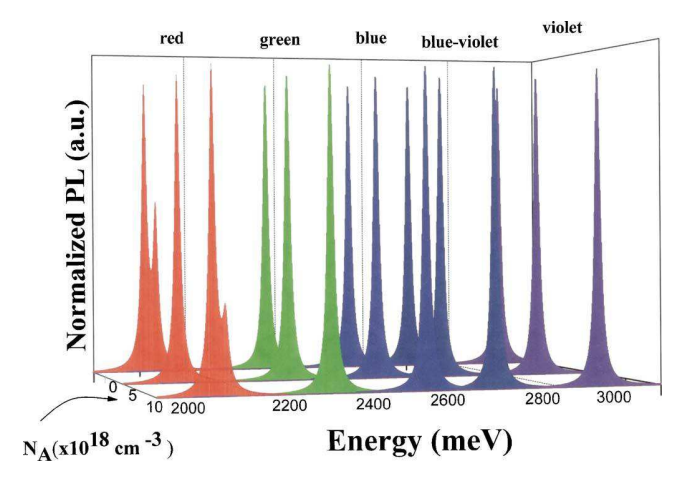


FIG. 2. Calculated normalized photoluminescence (PL) spectra, at T=2 K, for $(Al_{0.20}In_{0.05}Ga_{0.75})N/(Al_xIn_{1-x-y}Ga_y)N$ SLs, for x and y values as shown in Table II, for ionized acceptor concentrations of $N_A=0$, $N_A=5 \times 10^{18}$ cm⁻³, and $N_A=1\times 10^{19}$ cm⁻³. The energy range covers the electromagnetic spectrum from red to violet.

TABLE II. Values used for the alloy contents x and y in the p-doped cubic- $(Al_{0.20}In_{0.05}Ga_{0.75})N/(Al_xIn_{1-x-y}Ga_y)N$ SLs, properly chosen to attain light emission in the electromagnetic spectral regions indicated in the left column.

Cubic- $(Al_{0.20}In_{0.05}Ga_{0.75})N/(Al_xIn_{1-x-y}Ga_y)N$	х	у	1-x-y
Red	0.00	0.35	0.65
Green	0.02	0.40	0.58
Blue	0.08	0.45	0.47
Blue-violet	0.10	0.50	0.40
Violet	0.15	0.55	0.30

the main PL peak at the red region is related to recombination involving the second heavy-hole confined level.

In order to support the above interpretation, we analyze in more detail the spatial dependence of the different valence band edges for a particular case. We show in Fig. 4 the self-consistent hole subbands and potential profiles obtained for a p-doped SL emitting in the red, $(Al_{0.20}In_{0.05}Ga_{0.75})N/(In_{0.65}Ga_{0.35})N$, for $N_A = 5 \times 10^{18}$ cm⁻³. In the left-hand panel [Fig. 4(a)], the positions of the acceptor level in the barrier and the Fermi level along the SL are also shown. On the right-hand panel of the figure [Fig. 4(b)], the relative contributions for the total heavy-hole potential, V_{hh} , due to the Coulomb potential, V_C , and due to the exchange-correlation potential, V_{XC} , are compared. Although the acceptor level energy in the group-III nitrides is relatively deep, $\sim 200 \text{ meV}$ above the top of the valence band [as shown in Fig. 4(a), it is the strain effects due to lattice mismatch in the nitride-based SLs that assure the presence of rather deep potential wells, and the formation of a quasi-twodimensional hole gas (2DHG) which is confined inside them. Many-body effects such as exchange and correlation within the 2DHG have shown to be relevant, particularly for high hole-density systems. 13 As emphasized in Fig. 4(b), the exchange-correlation potential plays the major role, as compared to the Coulomb potential, and therefore it is responsible for the increase in the final potential well depth. Since the effects of exchange-correlation, as described in LDA, have been taken into account in the present calculations, the observed redshift of the spectra may be attributed mostly to the band gap renormalization (BGR).²⁵ This quantity can be extracted directly from the results shown in Fig. 4(b) by

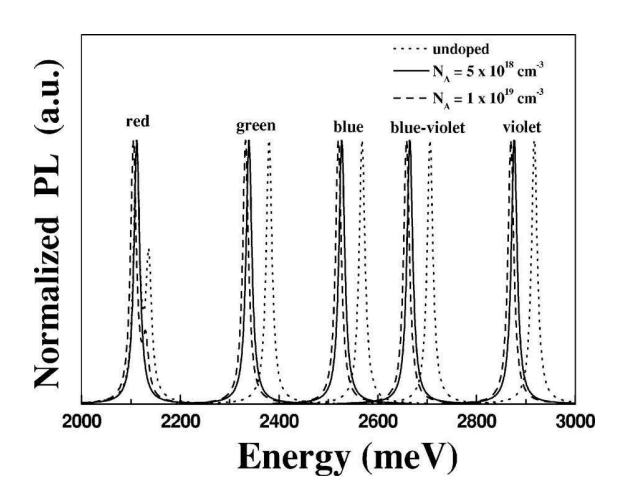


FIG. 3. PL spectra of Fig. 2, viewed in a two-dimensional picture in which different kinds of lines are ascribed depending on the doping case: undoped (dotted lines), $N_A = 5 \times 10^{18} \text{ cm}^{-3}$ (solid lines), and $N_A = 1 \times 10^{19} \text{ cm}^{-3}$ (dashed lines).

taking the energy difference BGR= V_{hh} - V_C^{hh} = V_{XC}^{hh} , which gives values varying between 20 and 47 meV.

The temperature dependence of the theoretical PL spectra is shown in Fig. 5 for one of the systems, a p-doped $(Al_{0.20}In_{0.05}Ga_{0.75})N/(Al_xIn_{1-x-y}Ga_y)N$ SL which emits in the blue (see Table II) for N_A =5×10¹⁸ cm⁻³. At low temperatures, the PL peaks remain practically unchanged. Above T=80 K, there is a significant redshift, and a second lessintense peak appears. This second peak arises from recombination involving excited hole states, with higher energies in the valence band. The relative intensity of this second peak enhances as T is increased. The energy difference between the fundamental and first excited electron states prevents the recombination from the latter.

Figure 6 illustrates the calculated PL and absorption spectra, at T=2 K, for a p-doped $(Al_{0.20}In_{0.05}Ga_{0.75})N/(Al_xIn_{1-x-y}Ga_y)N$ SL, which emits in the blue (see Table II) for $N_A=0$ (undoped), $N_A=5 \times 10^{18}$ cm⁻³, and $N_A=1\times 10^{19}$ cm⁻³. We clearly see a redshift in both the PL and absorption spectra, with the increase in N_A , which is caused by the enhancement of the hole's confinement. We can also extract from the calculations the

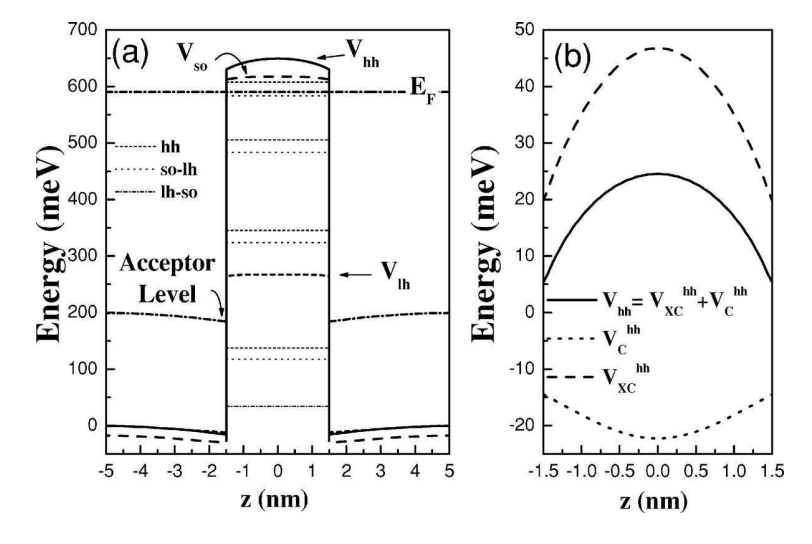


FIG. 4. p-doped (Al_{0.20}In_{0.05}Ga_{0.75})N/(In_{0.65}Ga_{0.35})N SL, with N_A =5×10¹⁸ cm⁻³, which emits in the red: (a) Real-space energy diagram showing the spatial dependence of the valence band edges for heavy (V_{hh}), light (V_{th}), and split-off (V_{so}) hole bands. Eight energy hole levels inside the well are depicted. Also shown, by thick dash-dotted lines, are the acceptor level in the barrier and the position of the Fermi level, E_F . The energy zero was taken at the top of the Coulomb potential at the barrier; (b) Different contributions to the self-consistent total heavy-hole potential (V_{hh}), due to the Coulomb (V_{C}^{hh}) and due to the exchange-correlation (V_{XC}^{hh}) potentials.

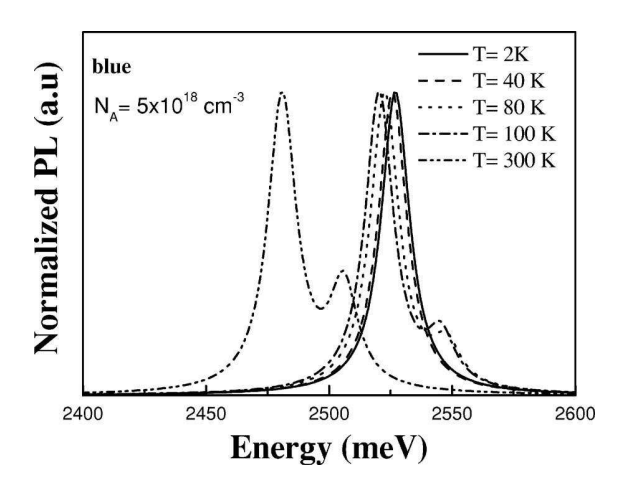


FIG. 5. Temperature dependence of the normalized calculated PL spectra, as obtained for a p-doped (Al $_{0.20}$ In $_{0.05}$ Ga $_{0.75}$)N/(Al $_x$ In $_{1-x-y}$ Ga $_y$)N SL which emits in the blue (see Table II). N_A =5 × 10¹⁸ cm $^{-3}$. Above T=80 K, a second less-intense peak appears, which is ascribed to recombination involving the first excited hole state.

values obtained for the Stokes shift, taken here as the energy difference between the PL peak and the absorption edge. We notice a significant increase in the values of the Stokes shifts as N_A increases, due to the many-body effects within the 2DHG present in these systems.

The values encountered for the Stokes shifts in the systems shown in Fig. 5 are approximately 20 and 40 meV, respectively, for $N_A = 5 \times 10^{18}$ cm⁻³ and $N_A = 1 \times 10^{19}$ cm⁻³. Similar values for the Stokes shifts have been found for p-doped ternary (AlGa)N/GaN SLs.²⁶

IV. CONCLUSIONS

We presented the band structure and light emission spectra calculations from p-doped quaternary $(Al_{0.20}In_{0.05}Ga_{0.75})N/(Al_xIn_{1-x-y}Ga_y)N$ SLs in the zinc blend structure, by using effective-mass theory and the $\mathbf{k} \cdot \mathbf{p}$ approach. The full eight-band Kane Hamiltonian, together with the Poisson equation, was solved, providing self-consistent potential profiles and hole's charge distributions for different SLs.

The alloy contents in the wells, x and y, as well as the acceptor doping concentration N_A in the barriers, have been varied. The light emission from the systems cover a wide range of the electromagnetic spectrum from violet through red, and can be precisely engineered by choosing proper x and y values for the molar fractions in the quaternary alloy.

The results obtained for the calculated luminescence and absorption spectra have proven that light emission arising from confined states recombination in the wells is redshifted in the doped SLs, when compared to the undoped case, and this behavior is caused by the potential bending induced by the presence of free holes in the SLs wells. Therefore, we demonstrated that it is feasible to achieve white light emission in *p*-doped quaternary III-nitride SLs, through proper engineering of the alloy molar fractions, which brings up insights toward advanced optoelectronic device technology development.

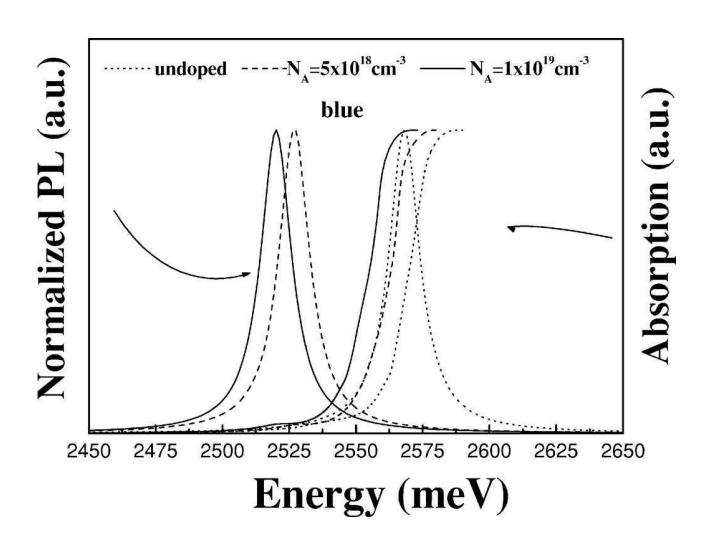


FIG. 6. Calculated PL and absorption spectra, at T=2 K, for a p-doped (Al $_{0.20}$ In $_{0.05}$ Ga $_{0.75}$)N/(Al $_{x}$ In $_{1-x-y}$ Ga $_{y}$)N SL, which emits in the blue (see Table II), for $N_{A}=0$ (undoped), $N_{A}=5\times10^{18}$ cm $^{-3}$, and $N_{A}=1\times10^{19}$ cm $^{-3}$.

ACKNOWLEDGMENTS

We acknowledge the Brazilian funding agencies FAPESP and CNPq for support. The author S.C.P.R. would like to express special thanks to CT-ENERG/CNPq for Grant 503.570/03–6, and E.F.S., Jr. also thanks CT-ENERG/CNPq for Grant 400.601/04–4. We would like to thank Professor D. J. As, from Paderborn University, Germany, for a critical reading of the manuscript, and for his suggestions.

O. Ambacher, J. Phys. D 31, 2653 (1998).

²P. Kung and M. Razegui, Opto-Electron. Rev. **8**, 201 (2000).

³H. Hirayama, J. Appl. Phys. **97**, 091101 (2005).

⁴Y. Taniyasu, M. Kasu, and T. Makimoto, Nature 441, 325 (2006).

⁵A. Khan, Nature **441**, 299 (2006).

⁶I. D. Goepfert, E. F. Schubert, A. Osinsky, P. E. Norris, and N. N. Faleev, J. Appl. Phys. 88, 2030 (2000).

⁷K. Kumakura, T. Makimoto, and N. Kobayashi, Jpn. J. Appl. Phys., Part 1 **39**, 2428 (2000).

⁸D. J. As, in *Optoelectronic Properties of Semiconductors and Superlattices*, edited by M. O. Manasreh (Taylor and Francis, New York, 2003), Vol. 19, p. 323.

⁹D. J. As, D. Schikora, and K. Lischka, Phys. Status Solidi C **0**, 1607

¹⁰L. M. R. Scolfaro, L. K. Teles, M. Marques, L. G. Ferreira, and J. R. Leite, in *Phase Separation and Ordering in Cubic Ternary and Quaternary Nitride Alloys*, edited by M. Henini and M. Razegui (Elsevier, Amsterdam, 2004).

¹¹J. Schörmann, S. Potthast, M. Schnietz, S. F. Li, D. J. As, and K. Lischka, Phys. Status Solidi C 3, 1604 (2006).

¹²A. Tabata, L. K. Teles, L. M. R. Scolfaro, J. R. Leite, T. Frey, A. Kharchenko, D. J. As, D. Schikora, K. Lischka, and J. Furthmüller, and F. Bechstedt, Appl. Phys. Lett. 80, 769 (2002).

¹³S. C. P. Rodrigues, G. M. Sipahi, L. M. R. Scolfaro, and J. R. Leite, J. Phys.: Condens. Matter **14**, 5813 (2002).

¹⁴S. C. P. Rodrigues, G. M. Sipahi, L. M. R. Scolfaro, J. R. Leite, T. Frey, D. J. As, D. Schikora, and K. Lischka, Phys. Status Solidi A 190, 121 (2002).

¹⁵M. Marques, L. K. Teles, L. M. R. Scolfaro, J. R. Leite, J. Furthmüller, and F. Bechstedt, Appl. Phys. Lett. 83, 890 (2003).

¹⁶U. Kohler, D. J. As, S. Potthast, A. Khartchenko, K. Lischka, O. C. Noriega, E. A. Meneses, A. Tabata, S. C. P. Rodrigues, L. M. R. Scolfaro, G. M. Sipahi, and J. R. Leite, Phys. Status Solidi A 192, 129 (2002).

¹⁷Y. Ishitani, M. Fujiwra, T. Shinada, X. Wang, S. Che, and A. Yoshikawa, International Workshop on Nitride Semiconductors 2006, 22–27 October, Kyoto, Japan.

¹⁸J. Schörmann, D. J. As, K. Lischka, P. Schley, R. Goldhahn, S. F. Li, W. Löffler, M. Hetterich, and H. Kalt, Appl. Phys. Lett. 89, 261903 (2006).

- ¹⁹S. P. Fu, T. T. Chen, and Y. F. Chen, Semicond. Sci. Technol. **21**, 244 (2006)
- (2006).

 ²⁰W. Walukiewicz, J. W. Ager III, K. M. Yu, Z. Liliental-Weber, J. Wu, S. X. Li, R. E. Jones, and J. D. Denlinger, J. Phys. D **39**, R83 (2006).
- ²¹F. Bechstedt, J. Furthmüller, M. Ferhat, L. K. Teles, L. M. R. Scolfaro, J. R. Leite, V. Yu. Davidov, O. Ambacher, and R. Goldhahn, Phys. Status Solidi A 195, 628 (2003).
- L. E. Ramos, L. K. Teles, L. M. R. Scolfaro, J. L. P. Castineira, A. L. Rosa, and J. R. Leite, Phys. Rev. B 63, 165210 (2001).
- ²³S. C. P. Rodrigues, L. M. R. Scolfaro, J. R. Leite, and G. M. Sipahi, Appl. Phys. Lett. **76**, 1015 (2000).
- ²⁴V. Yu. Davydov, A. A. Klochikhin, R. P. Seisyan, V. V. Emtsev, S. V. Ivanov, F. Bechstedt, J. Furthmüller, H. Harima, A. V. Mudryi, J. Aderhold, O. Semchinova, and J. Graul, Phys. Status Solidi B 229, R1 (2002).
- ²⁵D. A. Kleinman and R. C. Miller, Phys. Rev. B **32**, 2266 (1985).
- ²⁶S. C. P. Rodrigues, L. M. R. Scolfaro, G. M. Sipahi, and J. R. Leite, Phys. Status Solidi B **234**, 906 (2002).